J. Fluid Mech. (1984), vol. 139, pp. 325–345
Printed in Great Britain

On the detection of turbulence-generating events

By P. HENRIK ALFREDSSON AND ARNE V. JOHANSSON
Department of Mechanics, The Royal Institute of Technology, S-100 44 Stockholm, Sweden

(Received 13 September 1982 and in revised form 12 October 1983)

The structure of turbulence, especially in the near-wall region, was studied with the variable-interval time-averaging (VITA) technique and the uv-quadrant method. Both methods were applied to the same set of data, measured in a fully developed turbulent channel flow, to detect events associated with turbulence production. A close correspondence was found between VITA events and ejection type of events detected with the uv-quadrant method. Conditional averages of the fluctuating component of the streamwise velocity (u) and the component normal to the wall (v), as well as of the product uv, were constructed with both methods, and the cause for some of the apparent differences was investigated. In contrast to previous findings it was concluded that the uv-pattern obtained with the VITA technique has only one peak, and hence is quite similar to that obtained with the uv-quadrant method. It was shown that large peaks in the uv-signal (with $u < 0$, $v > 0$) imply large instantaneous outflow angles. For typical VITA events the outflow angle was often found to exceed 10°. Some events with large uv-peaks did not correspond to any strong activity in the u-component, but could be detected by applying the VITA technique to the v-signal.

1. Introduction

Organized structures in turbulent flows have been extensively investigated during the last decade (see e.g. Antonia 1981). From visual studies (Kline *et al.* 1967; Kim, Kline & Reynolds 1971; Corino & Brodkey 1969) it was discovered that a major part of the turbulence production occurs during short periods of 'violent' activity ('bursting' periods). These events take place close to the solid surfaces in wall-bounded shear flows (pipe, channel and boundary-layer flows). Several methods have been devised to detect these events from turbulent signals. The relevance of such burst detection schemes can be judged from their ability to detect events associated with significant contributions to the Reynolds stress.

Wallace, Eckelmann & Brodkey (1972) studied four classes of motions related to the four quadrants of the (u, v)-plane, thereby introducing the quadrant-splitting approach. Lu & Willmarth (1973) later extended this approach, by employing a threshold level, to sort out 'violent' events. This will in the following be referred to as the uv-quadrant method. It was used by Comte-Bellot, Sabot & Saleh (1978) to construct conditional averages of u, v and uv in the outer region of turbulent pipe flow.

The VITA technique, developed by Blackwelder & Kaplan (1976) is perhaps the most widely used detection method. They applied this technique to the streamwise velocity and showed that the detected events are associated with considerable contributions to the Reynolds stress. Chen & Blackwelder (1978) applied it, together with a slope criterion, to the temperature signal in a slightly heated boundary layer.

Johansson & Alfredsson (1982) studied the two different types of events, accelerations and retardations, detected in the streamwise velocity signal, and showed that the VITA technique singles out events with a duration which is roughly equal to the averaging time used in the detection criterion.

Wallace, Brodkey & Eckelmann (1977) developed a pattern-recognition technique, with which they obtained conditional averages characterized by a relatively slow decrease of the streamwise velocity followed by a rapid acceleration. The acceleration phase was shown by Eckelmann & Wallace (1980), to have some properties in common with the conditional averages obtained by Blackwelder & Kaplan (1976). However, the peak values of the uv-patterns for this method do not significantly exceed the long-time mean value.

Although the various schemes have all been devised to focus on the 'bursting' events, the outcome in form of conditional averages depends strongly on the specific detection criterion. This immediately raises the important question whether this is due to differences in the setting of reference times and other details in the conditional averaging process, or if the various methods detect distinctly different types of events. Studies of the relation between results obtained with various techniques are, however, scarce. Offen & Kline (1973) made simultaneous dye-visualization and hot-film measurements in a water channel, and compared results obtained with different detection schemes, among them the VITA and uv-quadrant methods, with the visual observations. However, in order to match the number of 'bursts' that were visually observed with the number of detections they had to use rather low threshold levels. This may be due to the fact that the field of view was larger than the extent of the probe, and hence not all the visually observed events passed across the probe. For the VITA method this low threshold resulted in a uv-pattern of almost negligible amplitude, in contrast with the findings of Blackwelder & Kaplan (1976).

Subramanian *et al.* (1982) have recently reported a comparison between the VITA and uv-quadrant methods. They applied the VITA technique to the temperature signal in a slightly heated boundary layer. The conditional averages of the uv-signal has a relatively small amplitude, which may partly be due to the low threshold used. The conditional averages obtained with the uv-quadrant method and the VITA technique were found to differ considerably. They also made a study similar to that of Offen & Kline (1973) by using a rake consisting of 10 temperature-sensitive probes as their reference. When a temperature front was identified across the boundary layer an event was considered to take place. An X-probe was used for the VITA and uv-quadrant detections, with the parameters tuned to obtain the same number of events per unit time as with the rake. The correspondence was generally found to be rather weak. At $y^+ = 40$ (y is the distance normal to the wall)† it was 42% for the VITA technique and only 15% for the uv-quadrant method. This may be explained by the large spanwise separation ($280l_*$) between the rake and the X-probe used to provide data for the detection schemes.

The purpose of the present work is to study the structure of turbulence in the near-wall region with the VITA method and the uv-quadrant method, and to investigate the cause for some of the apparent differences between the conditional averages obtained with the two methods, as found in earlier studies. The experiments were carried out in a fully developed turbulent water-channel flow, and hot-film anemometry was used for the velocity measurements. A close correspondence was

† The viscous time- and lengthscales are defined as $t_* = \nu/u_\tau^2$ and $l_* = \nu/u_\tau$ respectively, where u_τ is the friction velocity, Quantities normalized with t_*, l_* and u_τ are denoted by superscript + in the usual fashion.

found between the VITA events detected in the u-signal, and the ejection type ($u < 0$, $v > 0$) of events detected with the uv-quadrant method. It was also shown that the double peak in the uv-pattern found by Blackwelder & Kaplan (1976) is a result of not separating the acceleration events from the retardations. It was concluded that the VITA method, if the two types of events are separated, gives velocity patterns that are closer to the actual realizations than does the uv-method. The VITA technique was also applied to the v-signal. The events detected in this way had a considerably smaller typical timescale (duration) than the u-signal events. This reflects the well-known fact that the v-signal has, in a relative sense, more high-frequency content than the u-signal.

2. Experimental procedure

The 0.4×0.08 m^2 water channel at the Department of Mechanics of The Royal Institute of Technology, Stockholm was used for the measurements. These were carried out 69 channel heights from the inlet of the 6 m long test section, where the flow is fully developed. A filtering and temperature control system ensured drift-free conditions for hot-film measurements. A DISA X-probe (model 55R61) was used for the main part of the experiments. The length L and diameter D of the X-probe sensors are 1.25 mm and 0.07 mm, respectively, and they are separated by 1.1 mm. Some measurements were also carried out with a TSI single probe (model 1261-10W, $L = 0.5$ mm, $D = 0.025$ mm). The DISA M01 anemometer system was used, and the probes were run at constant temperature with an overheat of 16 °C. The calibration of the probes was carried out in a submerged jet. A modified version of King's law, in which effects of free convection at low velocities are taken into account, was fitted to the calibration data. Further details of the flow facility and data acquisition procedure for single-probe measurements are given in Johansson & Alfredsson (1981, 1982).

During the X-probe measurements, time series of the two anemometer signals were collected, using simultaneous sampling, through the 12 bit A/D converter of a DEC MINC system (PDP 11/23). The sampling rate was 1 kHz, giving a time between samples of less than 0.1 in viscous units. The data were stored on floppy discs as consecutive differences (maximum 8 bits), thereby enabling storage of a data pair in one 16 bit word. For each measurement position 460000 such data pairs were collected.

The two anemometer output voltages were converted to effective cooling velocities from which the streamwise velocity and the velocity normal to the wall are readily inferred as (h.o.t. means higher-order terms)

$$U_{\text{meas}} = U + u + \text{h.o.t.}, \tag{2.1}$$

$$V_{\text{meas}} = \frac{1-k_1^2}{1+k_1^2} v + \text{h.o.t.}, \tag{2.2}$$

and the turbulent shear stress (per unit mass)

$$\overline{uv}_{\text{meas}} = \frac{1-k_1^2}{1+k_1^2} \overline{uv} + \text{h.o.t.}, \tag{2.3}$$

where U is the mean velocity and k_1 is the sensitivity coefficient along the sensor (see e.g. Champagne, Sleicher & Wehrmann 1967). In order to get a mean value of V_{meas} equal to zero it was necessary to adjust the calibration constants slightly. The

adjustment, however, was only 1.5 % of the original values as determined from the calibration procedure. U_{meas} and V_{meas} were transformed to integer form and the time series of the velocities were also stored as consecutive differences (16 bits/pair).

The relations above show that the sensitivity along the sensors may affect the measured value of the velocity component normal to the wall and hence also the value of uv. For turbulent channel flow the $\overline{uv}$-distribution is given by

$$-\frac{\overline{uv}}{u_\tau^2} = 1-\frac{y}{b}-\frac{\mathrm{d}U^+}{\mathrm{d}y^+}, \tag{2.4}$$

where b is half the channel width. Equations (2.3) and (2.4) then offer a possibility to determine k_1 (if u_τ is known). By using an air-channel flow facility, in which u_τ could be determined from pressure-drop measurements, Taslim, Kline & Moffat (1978) found that neither for hot wires nor for hot films could k_1 be considered negligible in air flows. The k_1 values found were 0.30 and 0.38 respectively. The latter would give a measured value of uv, approximately 25 % too low. However, for hot films used in liquids the situation seems to be somewhat different. Eckelmann (1970) measured the uv-distribution in an oil channel and found good agreement with the distribution determined from (2.4), assuming $k_1 = 0$. As will be shown in §3, the uv-values measured in the present study are about 5 % lower than those inferred from (2.4). This corresponds to a k_1 value of 0.16. However, all results in the following are given with $k_1 = 0$.

2.1. *Detection schemes*

The VITA technique, devised by Blackwelder & Kaplan (1976), is based on the intermittent character of the short-time variance of a turbulent signal. This quantity gives a local measure of the 'turbulent activity'. Although Blackwelder & Kaplan applied the technique to the streamwise velocity, it can be used to analyse any fluctuating signal. The short-time variance of a signal $g(t)$ is defined as

$$\mathrm{var}_g(t,T) = \frac{1}{T}\int_{t-\frac{1}{2}T}^{t+\frac{1}{2}T} g^2(s)\,\mathrm{d}s - \left(\frac{1}{T}\int_{t-\frac{1}{2}T}^{t+\frac{1}{2}T} g(s)\,\mathrm{d}s\right)^2.$$

When the averaging time T becomes large the right-hand side tends to g_{rms}^2. An event is considered to occur when the short-time variance exceeds kg_{rms}^2, where k is a chosen threshold level. As was demonstrated by Johansson & Alfredsson (1982), there is a close relation between the mean duration of the detected events and the averaging time. Once the reference times, taken as the midpoints of the events, have been determined a conditional average can be calculated as

$$\langle g(\tau)\rangle = \frac{1}{N}\sum_{j=1}^{N} g(t_j+\tau), \tag{2.5}$$

where N is the number of events and τ is a time coordinate relative to the reference time t_j. Two distinctly different types of events are detected with the VITA technique; namely those with increasing velocity and those with decreasing velocity at the detection time.

The uv-signal has an intermittent character, which can be used to detect events associated with turbulence production. In the uv-quadrant method, an event is considered to occur when the uv-signal exceeds a chosen threshold, i.e. when $|uv|/u_{\text{rms}}\,v_{\text{rms}} > H$. Four different types of events, corresponding to the four quadrants of the (u,v)-plane, can be distinguished. The reference time is taken as the midpoint of the event, and the ensemble averages are calculated according to (2.5).

As the uv-quadrant method uses the amplitude of uv in a direct comparison with the threshold, it is possible to predict the amplitude of the conditional average of uv, if the frequency of occurrence $n_i(H)$ is known (where i is the quadrant number). The probability density distribution for the amplitude of uv-peaks is then

$$P_i(H) = -\frac{1}{n_i(0)}\frac{\mathrm{d}n_i}{\mathrm{d}H}.$$

Assuming that the maximum value of uv for each event occurs at the detection time, one can now calculate the amplitude of the uv-pattern as

$$\frac{\langle uv\rangle_{\mathrm{peak}}}{u_{\mathrm{rms}}v_{\mathrm{rms}}} = \frac{\int_H^\infty H'P_i\,\mathrm{d}H'}{\int_H^\infty P_i\,\mathrm{d}H'} = H + \frac{1}{n_i(H)}\int_H^\infty n_i(H')\,\mathrm{d}H'. \tag{2.6}$$

As will be shown in §3.1, $n_i(H)$ can be approximated by

$$n_i(H) = A_i\mathrm{e}^{-a_iH}. \tag{2.7}$$

The relations (2.6) and (2.7) yield

$$\langle uv\rangle^*_{\mathrm{peak}} = \frac{\langle uv\rangle_{\mathrm{peak}}}{Hu_{\mathrm{rms}}v_{\mathrm{rms}}} = 1 + \frac{1}{a_iH}. \tag{2.8}$$

3. Results

To get an adequate comparison between results obtained with the VITA technique and the uv-quadrant method, the two detection schemes were applied to the same set of data taken at a Reynolds number of 15000 (based on centreline velocity U_{CL}, and channel height $2b$). The viscous (inner) scales (t_* and l_*) are 13.0 ms and 0.110 mm respectively, whereas the outer timescale b/U_{CL} is 229 ms. For this Reynolds number the extent of the X-probe sensors in the direction normal to the wall is $8l_*$, while they are $10l_*$ apart. To determine the friction velocity, u_τ and to check the mean statistics obtained with the X-probe, measurements were carried out at approximately the same Reynolds number with a single probe. This probe could be placed as close to the wall as $y^+ = 1.3$, and the friction velocity could be accurately determined from the linear velocity distribution in the viscous sublayer. The effect of heat conduction to the wall, which may give too-high velocity readings in the immediate vicinity of the wall, is small in this case, whereas it often causes severe problems in air flows. The U_{CL}/u_τ ratio was found to be 20.6, which was used to determine the friction velocity for the X-probe measurements.

The mean-velocity distributions measured with the two probes are presented in figure 1 (*a*). The logarithmic region is well described with the Kármán constant and the logarithmic intercept equal to 0.41 and 6.0 respectively. The turbulence intensity, skewness and flatness for the u and v velocity components are shown in figures 1 (*b–d*). There is reasonably good agreement between results obtained with the two probes, as well as with the results of Kreplin & Eckelmann (1979*b*), which are included for comparison in figures 1 (*b–d*). As pointed out by Eckelmann (1970), the maximum value of v_{rms}/u_τ is commonly found to be close to 1.0, which is also obtained in the present study. The v-component has a positive skewness and a high flatness factor in the near-wall region, suggesting the existence of intermittent ejections in this region.

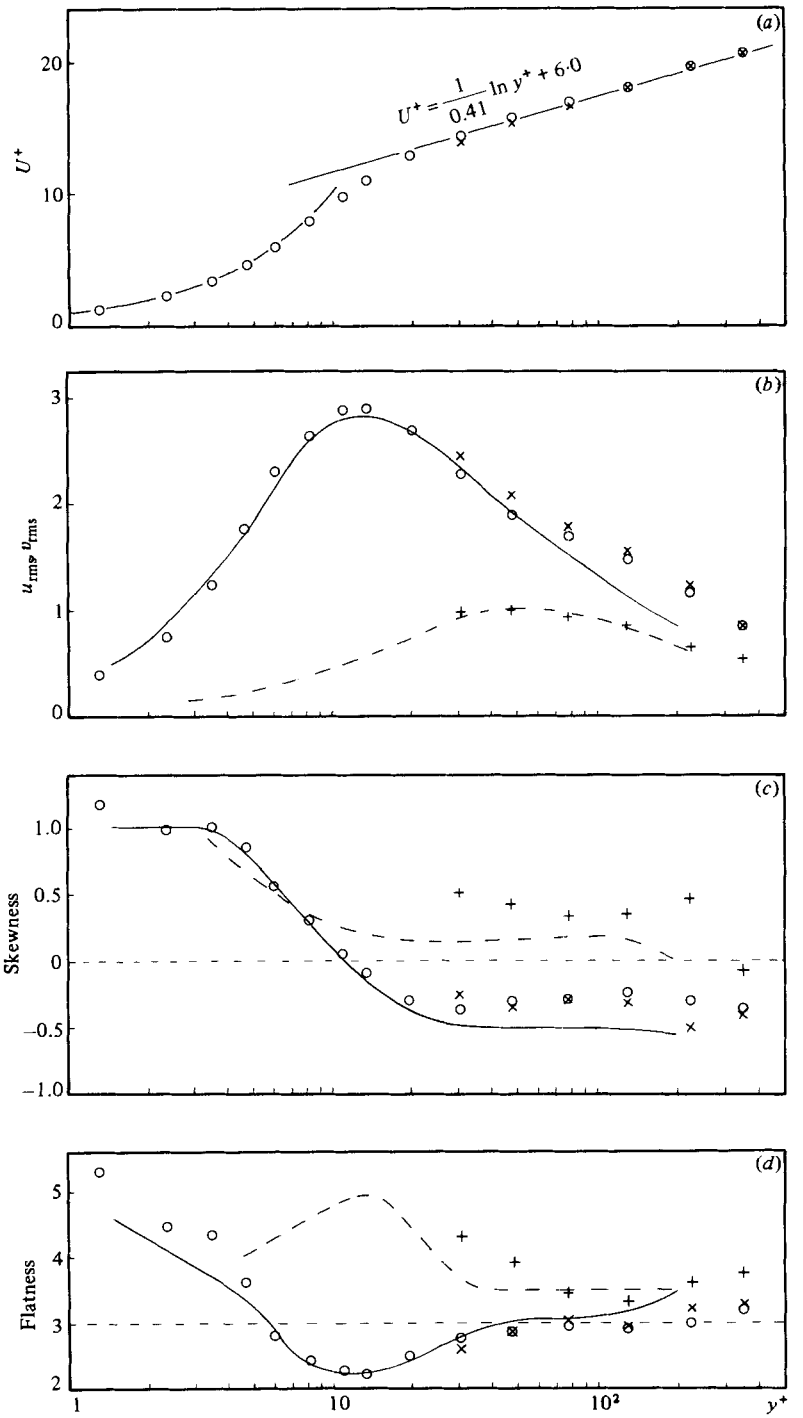

FIGURE 1. Distribution of the statistical moments measured with the X-probe (× for u, + for v) and the single probe (○): (*a*) mean velocity; (*b*) turbulence intensity; (*c*) skewness; (*d*) flatness. Data from Kreplin & Eckelmann (1979*b*) (*b–d*) and Eckelmann (1970) (*b*): ——, u; - - -, v.

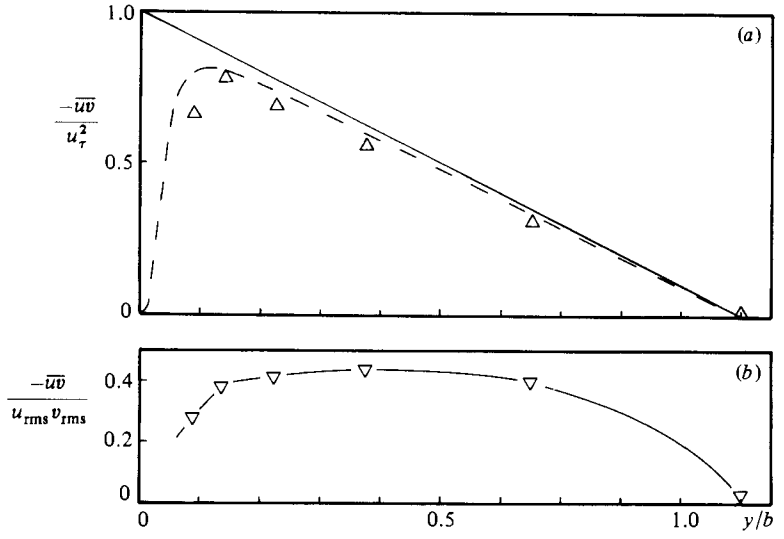

FIGURE 2. Distribution of the normalized Reynolds stress. (*a*) $\overline{uv}/u_\tau^2$: —, total shear stress; ---, Reynolds stress obtained from the mean-velocity distribution, (*b*) $\overline{uv}/u_{\rm rms}v_{\rm rms}$.

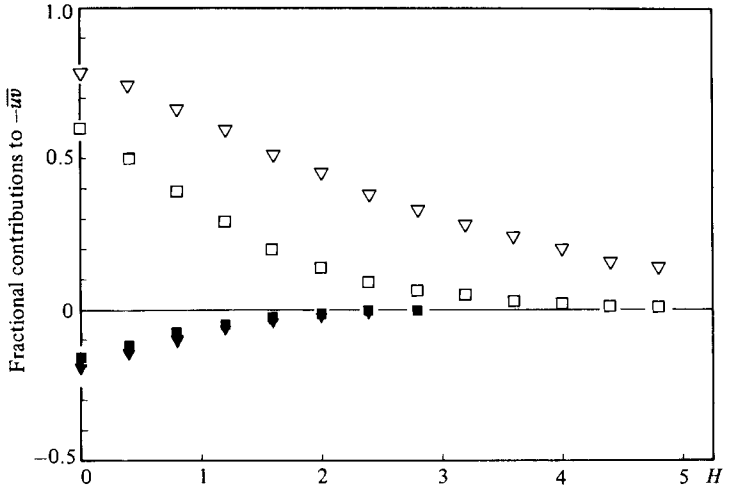

FIGURE 3. Contributions to $\overline{uv}$ from the different quadrants at $y^+ = 50$, as function of threshold level: ■, q1; ▽, q2; ▼, q3; □, q4.

The measured uv-distribution presented in figure 2 has values that are slightly lower (5 %) than those derived from (2.4) (with $\mathrm{d}U^+/\mathrm{d}y^+$ determined from the mean-velocity distribution measured with the single probe). This may be a result of the influence of the coefficient k_1, as discussed in §2. Also plotted is $-\overline{uv}/u_{\rm rms}v_{\rm rms}$, which has an almost constant value of 0.4 in the logarithmic region. This is in good agreement with the results of Eckelmann (1970). Note that this quantity is not affected (to the first order) by k_1. The main contribution to $\overline{uv}$ stems from the second quadrant for $y^+ > 15$ (see Brodkey, Wallace & Eckelmann 1974). At $y^+ = 50$, 78 % of the total mean originates from the second quadrant. This and the fractional contributions from the other quadrants agree closely with the results of Brodkey *et al.* It is seen in figure 3 that peaks in the uv-signal higher than $4u_{\rm rms}v_{\rm rms}$ are almost exclusively found in

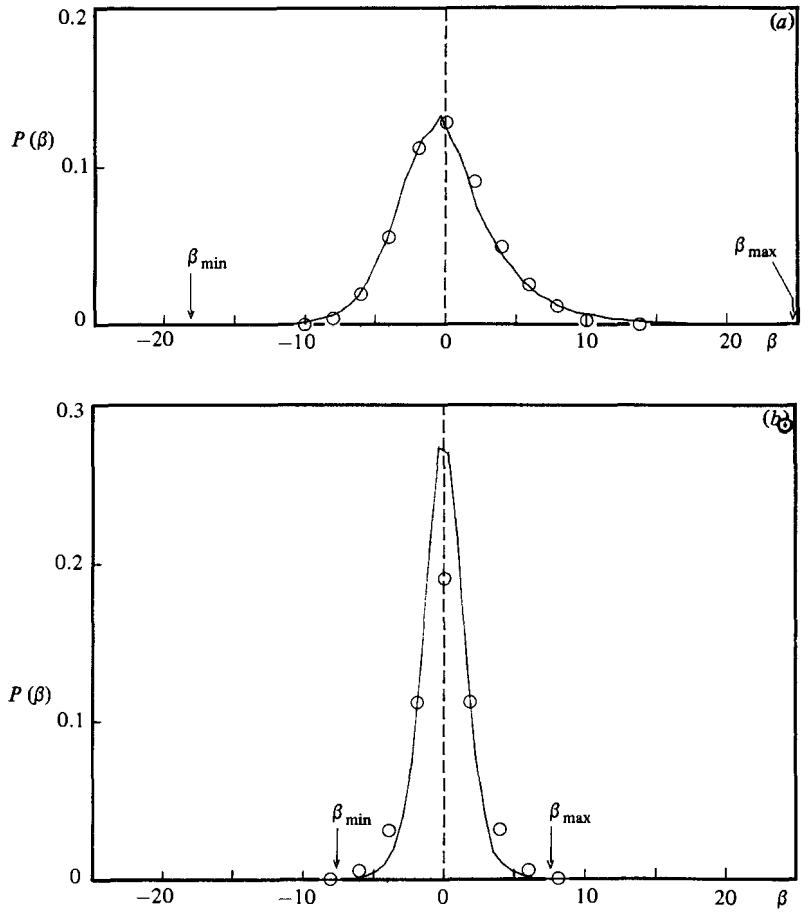

FIGURE 4. Probability density distributions of the instantaneous flow angle (in the (u, v)-plane): ○, data from Kreplin & Eckelmann (1979*a*); (*a*) $y^+ = 50$; (*b*) $y/b = 1$.

the second quadrant. These peaks contribute 20 % of the Reynolds stress during only 1.5 % of the total time.

It can readily be shown that, for a given amplitude of a uv-peak in the second quadrant, the following relation holds for the associated instantaneous outflow angle β:

$$\tan\beta > 4C/U^{+2}, \tag{3.1}$$

where $C = -uv/u_\tau^2$. Thus large peaks in the uv-signal (with $u < 0$, $v > 0$) imply large outflow angles. However, the reverse is not necessarily true. Willmarth & Lu (1972) made X-probe measurements in air (sensor separation = $16l_*$) and reported instantaneous values of uv as large as $62\overline{uv} \approx 50u_\tau^2$ at $y^+ = 30$, where the mean velocity U^+ was about 14. The relation (3.1) then yields that β must have been at least 45°, i.e. parallel to one of the X-probe sensors. The accuracy of these data must therefore be taken with some reservation. Such large values of uv (and corresponding angle) may be caused by large velocity gradients in the spanwise direction, as discussed by e.g. Willmarth & Bogar (1977). The maximum value of uv as measured (at $y^+ = 50$, $U^+ = 15.3$) in the present study was $26u_\tau^2$, with a corresponding outflow angle of 25° (satisfying the relation (3.1)).

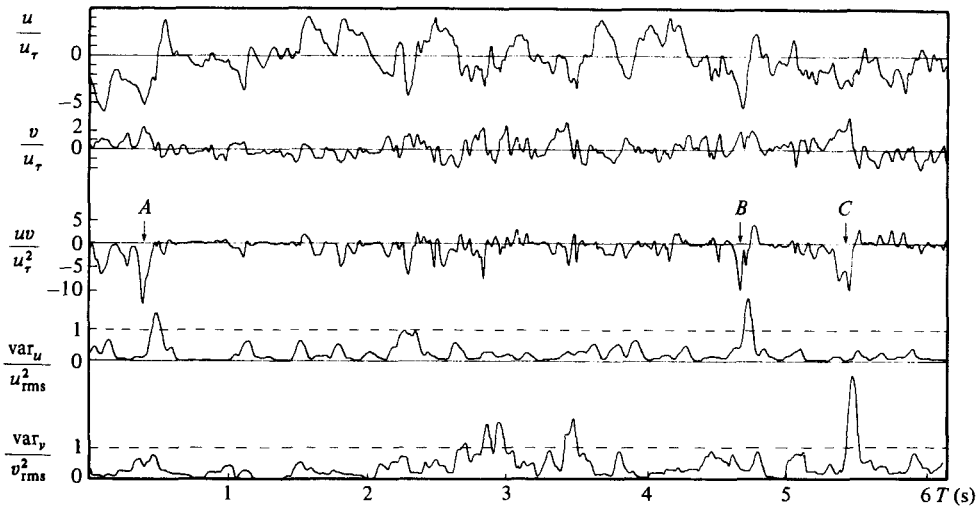

FIGURE 5. A portion of the u-, v- and uv-signals and the corresponding short-time variances of u and v for $T = 10t_*$.

Probability density distributions of the direction of the velocity vector in the uv-plane for the present study (at $y^+ = 50$ and $y/b = 1$) are shown in figures 4(a, b) together with the data of Kreplin & Eckelmann (1979a). At $y^+ = 50$ the overall agreement is good, although the extreme values found in the present study ($-18°$ and $+25°$) are almost twice as large as those of Kreplin & Eckelmann. However, Eckelmann (private communication) has pointed out inadequacies of the determination of the maximum flow angles in that paper. Hofbauer (1978) made visualization studies in the same channel flow as used by Kreplin & Eckelmann and found outflow angles ($v > 0$) of 25° and inflow angles of about 15° in the near-wall region. Large outflow angles (31°) were also reported by Nychas, Hershey & Brodkey (1973) for a turbulent boundary layer. In the present case, outflow angles larger than 12.5°, i.e. half the maximum value, occurred during only 1.0% of the total time. During this time, however, the contribution to the Reynolds stress was approximately 13%.

3.1. *Detection of events*

A portion of the u, v and uv-signals at $y^+ = 50$ is shown in figure 5. The uv-signal has an intermittent character, reflected in a high flatness factor of uv, which at this position is approximately 14. The skewness of uv has a large negative value (-2.3 at this position), which means that most large amplitude peaks in the uv-signal are negative. Also shown are the VITA variances of u and v, calculated with an averaging time of 10 viscous time units. Three peaks for which $-uv/u_\tau^2$ exceeds as high a level as 10, are found in this portion of the signal. At A and B these events are associated with large peaks in the short-time variance of u, both corresponding to accelerations. The uv-peaks are caused by a low streamwise velocity and a large velocity component away from the wall, i.e. an ejection, followed by a sharp increase in the streamwise velocity. Therefore the resulting peak in the short-time variance does not coincide in time with the peak in the uv-signal. At C the peak in the uv-signal is not associated with any strong activity in the streamwise velocity, but rather with a rapid change from a positive to a negative value of the v-component, giving a large value of the short-time variance of v. The events described above are all associated with relatively

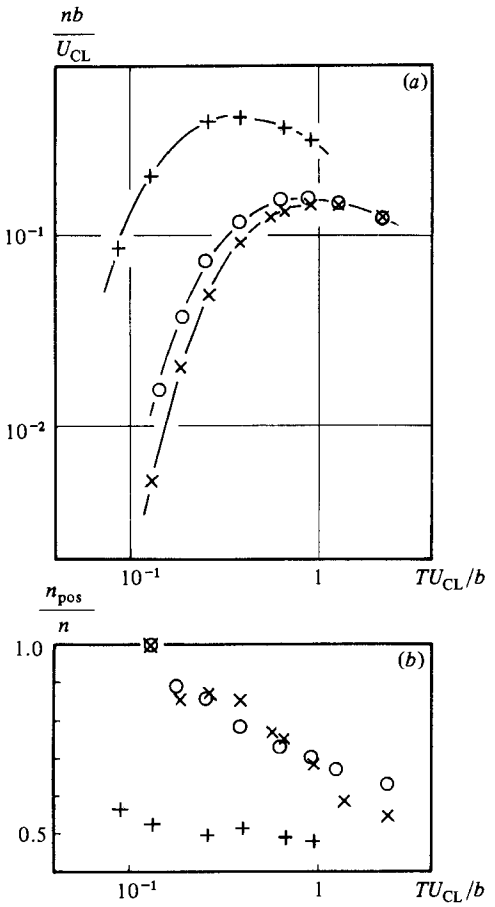

FIGURE 6. (*a*) The number of events detected per unit time with the VITA technique with $k = 1.0$, in the u-signal (○, single probe; ×, X-probe), and in the v-signal (+), as function of the averaging time. (*b*) Fraction of events with increasing velocity at the detection time; $y^+ = 50$.

large outflow angles. For the event at C the outflow angle is approximately 15°. In general, most of the large uv-peaks were found to be associated with ejection type of events. However, some rare sweep-type events ($u > 0$, $v < 0$) associated with a relatively large inflow angle and uv-peak were also observed.

As indicated in figure 5, more events are detected (with the VITA technique) in the v-signal than in the u-signal for the same threshold level. This was found to be true for all integration times (figure 6*a*) and threshold levels. For short averaging times most events detected in the u-signal correspond to accelerations. However, the events detected in the v-signal do not have a preferred sign of $\mathrm{d}v/\mathrm{d}t$ at the detection time. This is shown in figure 6 (*b*), where the fractional part of the events corresponding to an increase in the velocity (at the detection time) is plotted. Results for the single probe, which has a spanwise extent of $4.5l_*$, are included in figure 6 for comparison. The agreement is good, but some differences are seen for small values of T. However, the effects of finite sensor separation of the X-probe seem to be small for an averaging time of 10 viscous time units ($TU_{CL}/b = 0.57$), which was used for the conditional averages presented in the following.

Johansson & Alfredsson (1982) found that the mean duration of the detected events

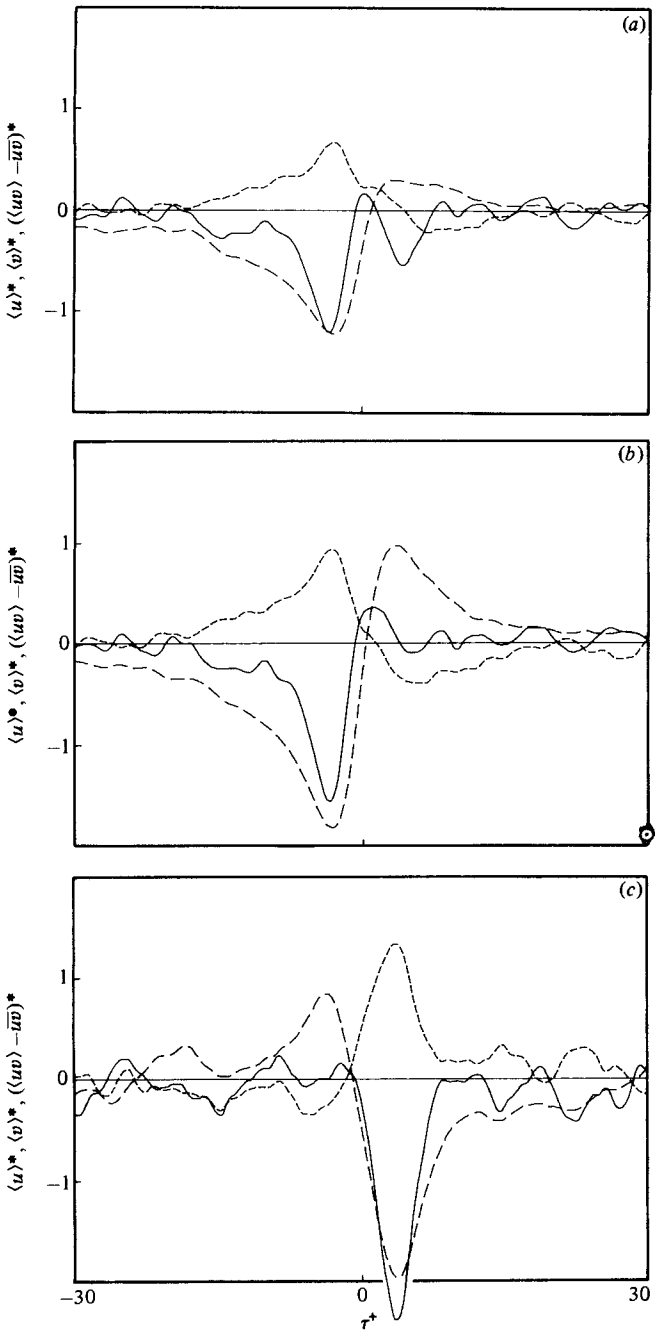

FIGURE 7. Conditional averages of u (——), v (- - -) and uv (——) for events, detected in the u-signal with the VITA method: (*a*) all events; (*b*) events with positive slope; (*c*) events with negative slope.

is roughly the same as the averaging time. Curves for the frequency of occurrence n versus the averaging time T therefore yield the timescale distribution of the events. To illustrate this further, take as a hypothetical example two fluctuating signals with identical statistical moments but one shifted a factor c in frequency with respect to the other. The frequency of occurrence would depend on the averaging time in the

same way for both cases. However, the high-frequency signal would have a larger maximum value of n located at a smaller T-value. The shifts in n and T would be factors c and $1/c$ respectively. Although the mean statistics of u and v are different, the above reasoning can be used to explain qualitatively the differences between the curves for u and v in figure 6(*a*). The turbulent energy of the fluctuations normal to the wall is found at higher frequencies than for the streamwise velocity fluctuations. The maximum number of events in the v-signal is consequently found for a shorter (about one-third) averaging time, whereas the number of detected events is about three times larger than for the u-signal.

Conditional averages were constructed from events detected with the VITA technique with and without slope criterion. The velocity patterns are normalized with the square root of the threshold times the respective r.m.s. value, whereas the uv-patterns are normalized with $ku_{\rm rms}v_{\rm rms}$ (non-dimensional quantities are denoted by an asterisk). The detection scheme was applied to both the u-signal and the v-signal, and the averaging time for both cases was 10 viscous time units, whereas the threshold k was 1.0. These data were taken at $y^+ = 50$; however, ensemble averages at $y^+ = 30$ have practically the same appearance. In figure 7(*a*) the detection was carried out in the u-signal without any slope criterion, and conditional averages of the u-, v- and uv-signals were calculated using the same reference times. The uv-pattern is seen to have two peaks, one before and one after the detection time. This was also found by Blackwelder & Kaplan (1976) at $y^+ = 15$. This double peak, as will be shown in the following, is a consequence of not separating the two types of events that are detected with the VITA technique. When they are treated separately (figures 7*b*, *c*) there is only one peak in the uv-pattern for each case, which is located at the time when $\langle u \rangle$ is a minimum. The v-pattern is seen to have a maximum at about the same time, which is ahead of the time of detection in case of an acceleration and after in the case of a retardation. It is obvious from this that an ensemble average of all events would have a double peak of the uv-pattern seen in figure 7(*a*). It may also be pointed out that the actual realizations observed in the uv-signal rarely exhibit the 'double-peak feature'. As seen from figures 7(*b*, *c*) the largest peak of $\langle uv \rangle$ is found for the retardation type of events. However, the acceleration type of events produce the largest contribution to the Reynolds stress because of the larger number of such events. Conditional averages constructed for other threshold levels showed that the amplitude of the u- and v-patterns scales well with the square root of k, whereas the amplitude of $\langle uv \rangle^*$ increases with increasing threshold. Hence, for low threshold levels, events are detected which are not associated with any significant turbulence production.

After the sharp increase of $\langle u \rangle$ in figure 7(*b*), as well as before the sharp decrease of $\langle u \rangle$ in figure 7(*c*), there is a period where $u > 0$ and $v < 0$, indicating a sweep type of motion. During this period, however, there is very little contribution to the Reynolds stress. The characteristics of the conditional averages in figure 7(*b*) would fit into a picture of these events as consisting of an ejection with relatively large outflow angle followed by a sweep type of motion of fluid approaching the wall at a small angle (cf. figure 12 of Eckelmann *et al.* 1977). An estimate of these angles from figure 7(*b*) yielded values of 4.6° and 1.6° respectively. Of course, these values increase with increasing threshold, e.g. for $k = 2.0$ the outflow angle was estimated to 7.5°. As previously mentioned, the actual realizations can have considerably larger angles.

The conditional averages shown in figures 8(*a–c*) were constructed from events detected in the v-signal. When both types of events are included in the ensemble averages (figure 8*a*) the resulting v-pattern is of very small amplitude since there are

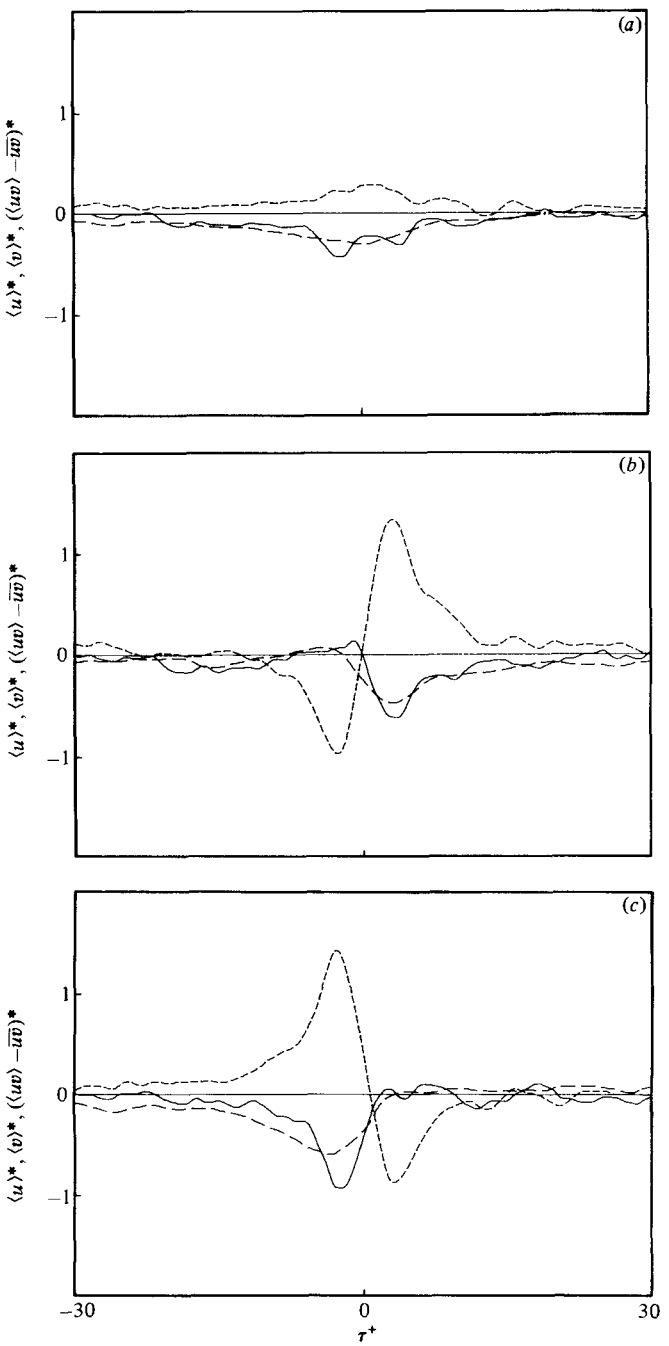

FIGURE 8. Conditional averages of u (– –), v (- - -) and uv (——) for events, detected in the v-signal with the VITA method: (*a*) all events; (*b*) events with positive slope; (*c*) events with negative slope.

equally many events of the two kinds. An artificial double peak in the uv-pattern is found also here. When the two kinds of events are separated (figures 8*b*, *c*) the v-patterns resemble those for u in figures 7 (*b*, *c*). The peak in the uv-patterns for the events detected in the v-signal is not as large (for the same threshold level) as for the events detected in the streamwise velocity. However, it is also were located at a time

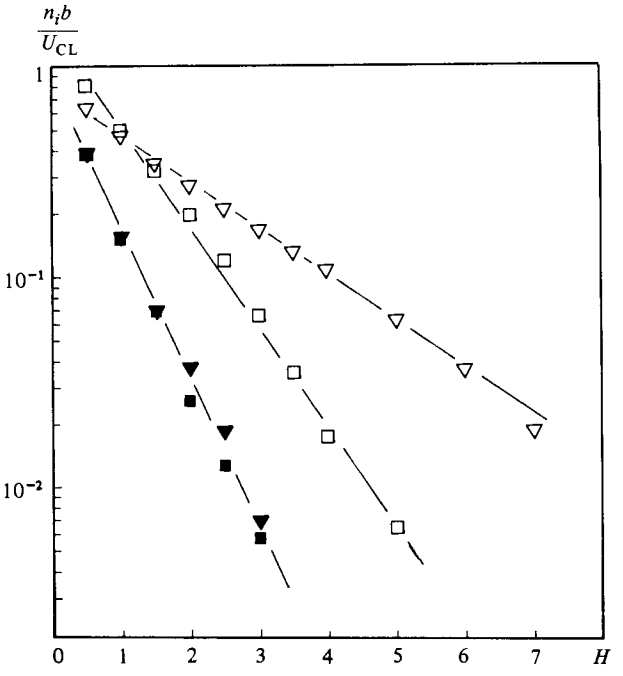

FIGURE 9. Number of events detected per unit time with the *uv*-quadrant method as function of the threshold level at $y^+ = 50$: ■, q1; ▽, q2; ▼, q3; □, q4.

when $\langle v \rangle$ is a maximum and $\langle u \rangle$ is a minimum. Hence the peak in the *uv*-pattern is for all these types of VITA events associated with ejection (lift-up) of low-speed fluid.

Both the VITA technique and the *uv*-quadrant method employ a threshold level in order to sort out events from the turbulent signal. For both methods the number of events detected decreases exponentially with the threshold (see Johansson & Alfredsson 1982). The lack of a unique threshold for which events may be said to occur implies of course that there is no well-defined value of the 'bursting frequency' obtained with either of these two methods. For the *uv*-quadrant method the rate of decrease is different for the four quadrants (figure 9), and the slowest decrease is found for events in the second quadrant, i.e. ejections. At a threshold of 4 there are six times as many ejections as sweeps, whereas practically no events were found in the first and third quadrants.

To investigate the correspondence between results obtained with the VITA technique and the *uv*-quadrant method, a comparison was carried out between VITA events detected in u with an averaging time of $10t_*$ and $k = 1.0$, and *uv*-peaks detected with $H = 4$. With these parameter values equally many events were detected with the two methods. About 50 % of the VITA events were found to be associated with a *uv*-peak larger than $4u_{\rm rms}v_{\rm rms}$ located within $25t_*$ from the detection time, while more than 90 % of them were associated with a *uv*-peak larger than $2u_{\rm rms}v_{\rm rms}$. The correspondence between VITA events and *uv*-peaks was about the same for other averaging times tested ($5t_*$ and $20t_*$). Both accelerations and retardations were in general associated with ejections. However, for almost all accelerations the *uv*-peak occurred prior to the VITA detection, whereas the opposite is true for the retardations (figure 10). The most-probable location of the *uv*-peak is approximately $3t_*$ before

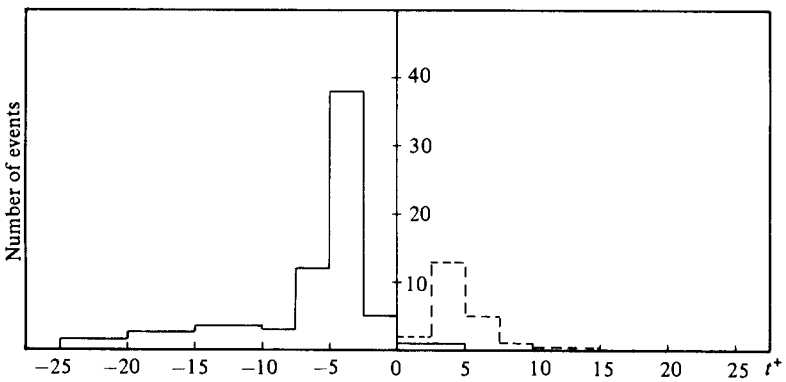

FIGURE 10. Distribution of the time delay between the VITA detection ($k = 1.0$, $T = 10t_*$) and the detection of an ejection, with the uv-quadrant method ($H = 4$): ——, accelerations; ---, retardations.

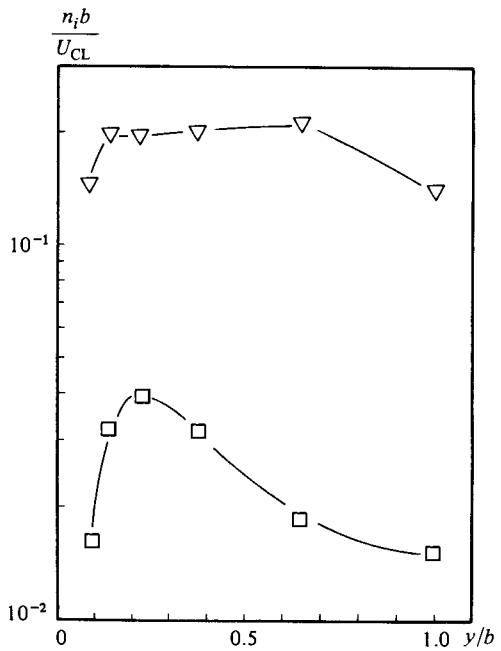

FIGURE 11. Number of events detected per unit time with the uv-quadrant method ($H = 4$) as function of y/b: ▽, q2; □, q4.

and after the detection time respectively. Offen & Kline (1973) made a similar study, but used a low threshold level without separating accelerations from retardations, and therefore did not observe the abovementioned features.

The ejections, as described by Corino & Brodkey (1969) and Kline *et al.* (1967) take place in the near-wall region. However, ejection-type as well as sweep-type motions which give large peaks in the uv-signal can be found also in the outer flow region, although there is as yet little evidence that these motions are related with the events observed close to the wall. The distributions of sweeps and ejections detected with the uv-quadrant method ($H = 4$) across the channel are shown in figure 11. It can be noted that the distribution of ejections is rather uniform in the region where $\overline{uv}/u_{\text{rms}}v_{\text{rms}}$ is approximately constant (figure 2*b*). The distribution of sweeps has a

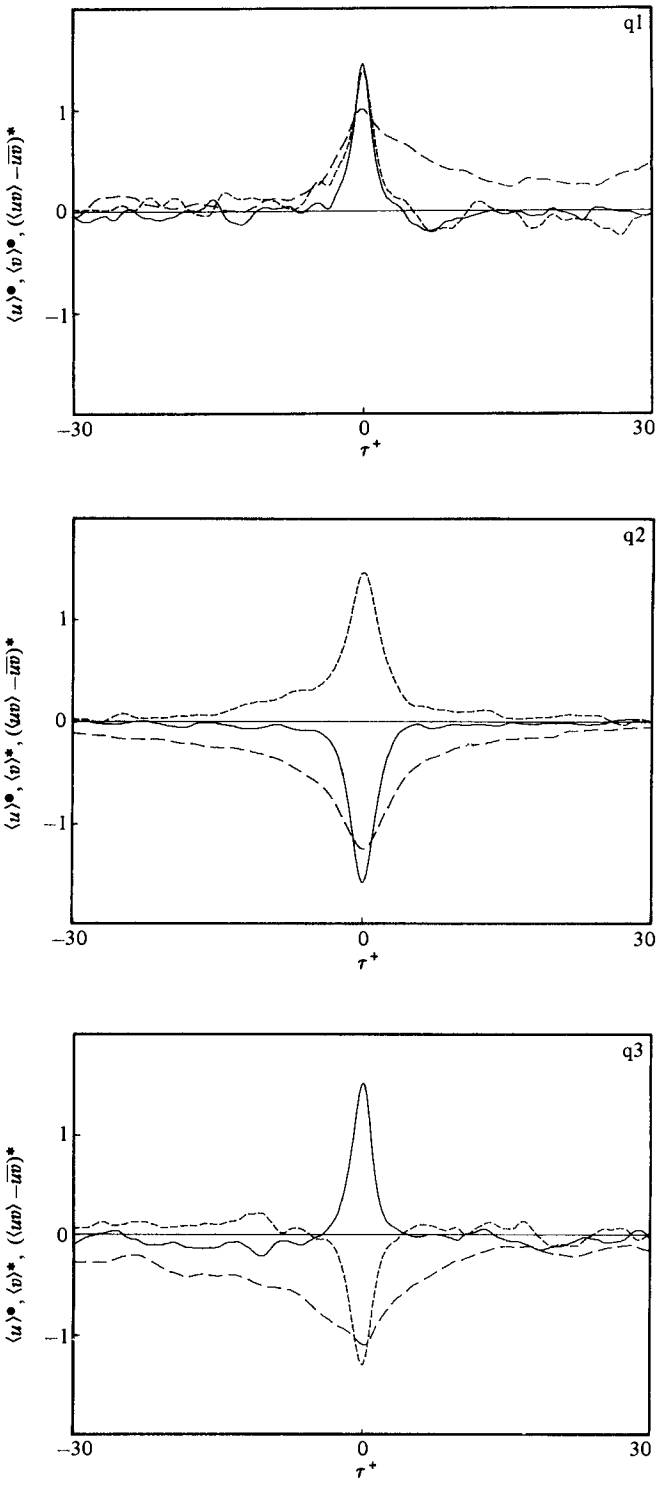

FIGURE 12. For caption see facing page.

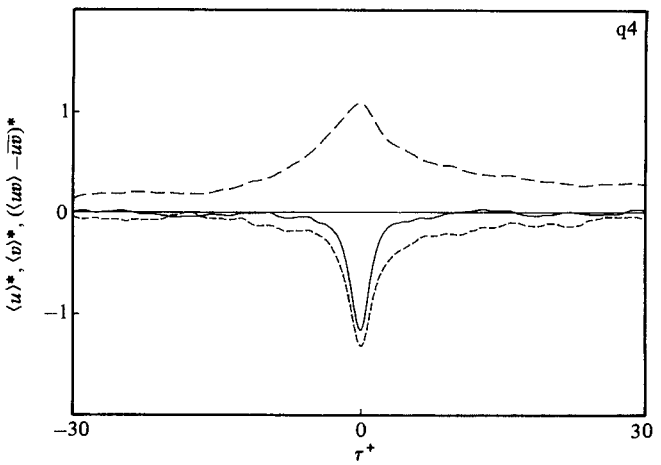

FIGURE 12. Conditional averages of u (– –), v (- - -) and uv (——) for the four types of events detected with the uv-quadrant method; $H = 2$, $y^+ = 50$.

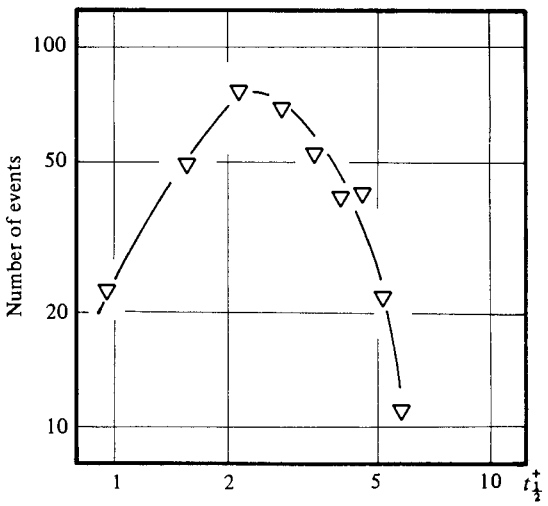

FIGURE 13. Halfwidth duration of uv-peaks larger than $2u_{\rm rms}v_{\rm rms}$ (q2, $y^+ = 50$).

peak at about $y^+ = 75$ ($y/b \approx 0.2$), which is in the region where most sweeps were observed in the visual study of Nychas *et al.* (1973).

Conditional averages of u, v and uv for the four different types of events detected with the uv-quadrant method (at $y^+ = 50$, $H = 2$) have their extreme values close to the detection time (figure 12). The peak in the u-pattern is wider than for $\langle v\rangle$, which is expected since the most probable duration is shorter for the VITA events detected in the v-signal than for the u-signal events (figure 6*a*). The width at halfheight of the v-pattern, for the events in the second quadrant, is about 4 viscous time units, which is about half of that for the u-pattern. The width of the uv-pattern is slightly less than that of $\langle v\rangle$. Notable is the asymmetrical appearance of the u-patterns in the first and third ('interaction') quadrants.

These ensemble averages give a mean value of the uv-peak duration. The distribution of the halfwidth duration (i.e. the width at half the maximum amplitude)

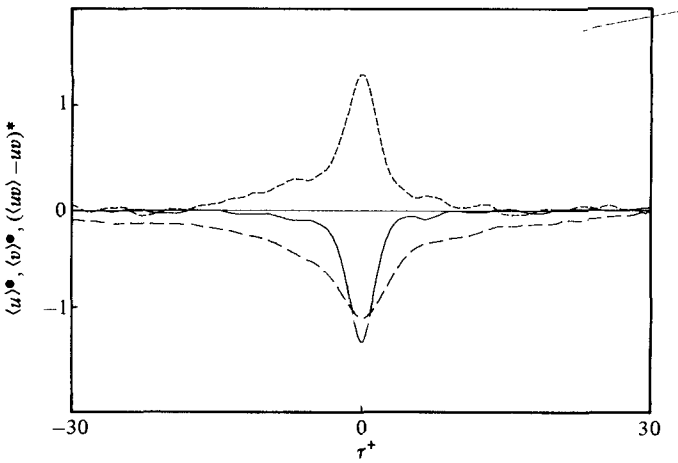

FIGURE 14. Conditional averages of u (--), v (- - -) and uv (——) for events detected in quadrant 2; $H = 4$, $y^+ = 50$.

i	a_i	H	Calculated peak	Measured peak
1	1.66	2.0	1.3	1.3
2	0.86	2.0	1.6	1.8
	—	4.0	1.3	1.4
3	1.66	2.0	1.3	1.3
4	1.10	2.0	1.5	1.4

TABLE 1. A comparison between calculated and measured peaks of $\langle uv\rangle^*$

of individual uv-peaks larger than $2u_{\rm rms}v_{\rm rms}$ was also determined, and is shown in figure 13. This distribution is narrower than that of VITA events, and has its maximum value at as small a value of the halfwidth as $2t_*$. The mean value is somewhat larger, about $3t_*$, which is close to that estimated from conditional averages obtained both with the VITA and the uv-quadrant methods.

Conditional averages for events detected with a high threshold ($H = 4$) in the second quadrant are shown in figure 14. The appearance is qualitatively the same as for $H = 2$. The peak values of $\langle uv\rangle^*$ as found in figures 12 and 14 are compared in table 1 with those calculated from the relation (2.8). The agreement between calculated and measured peak values of $\langle uv\rangle^*$ is good, which reflects the fact that $n_i(H)$ is well described by $e^{-a_i H}$.

Conditional averages of ejection type of events at $y/b = 0.375$ are shown in figure 15. The patterns closely resemble those found closer to the wall. Also included is the uv-pattern from Comte-Bellot *et al.* (1979)† for pipe flow at $y/R = 0.4$ (R is the pipe radius) with a Reynolds number of 135000. The width at halfheight of the uv-pattern is seen to be about a factor of three larger, in viscous units, for their case. In outer units it is about a factor of two smaller. Hence the duration of the uv-patterns seems to scale neither with inner nor with outer variables, at this position. One should, however, be aware of the differences in flow situation between the two cases. The

† Their pattern has been shifted in time because of differences in the setting of the reference times.

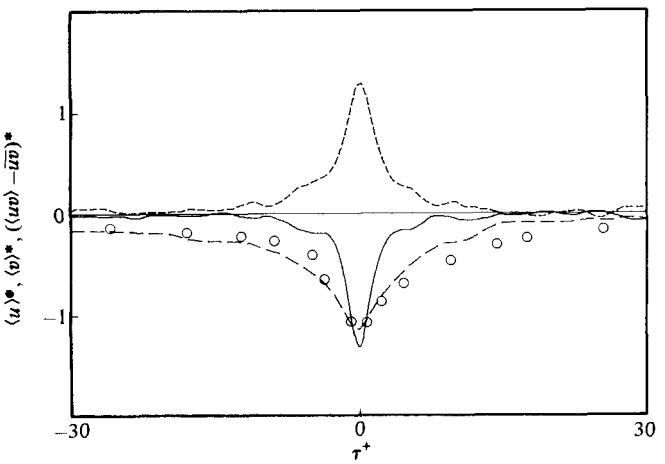

FIGURE 15. Conditional averages of u (——), v (- - -) and uv (——) for events detected in quadrant 2; $H = 4$, $y/b = 0.375$: ○, uv-pattern from Comte-Bellot *et al.* (1979), $H = 4$, $y/R = 0.40$, $Re = 135000$.

frequency of occurrence, for $H = 4$, is for their case 0.18 when normalized with the outer timescale. This is close to the value (0.20) obtained in the present study.

4. Discussion and conclusions

The events detected with the uv-quadrant method as well as with the VITA technique, using high threshold levels, are in general associated with an ejection type of motion ($u < 0$, $v > 0$). The uv-peaks (at $y^+ = 50$) with an amplitude larger than $4u_{\rm rms}v_{\rm rms}$, i.e. about 10 times the long-time mean value, are almost exclusively ejections. Such large amplitudes occur during only 1.5 % of the total time, but contribute more than 20 % of the Reynolds stress. The frequency of occurrence of such peaks is about the same as for events detected with the VITA technique (in the u-signal) with $k = 1.0$ and $T = 10t_*$. About 50 % of these VITA events were directly associated with a uv-peak detected with $H = 4$, and more than 90 % of them had a uv-peak detected with $H = 2$. The uv-peaks, however, do not coincide with the detection times obtained with the VITA technique, but are for accelerations, in general occurring prior to the VITA detection. The most probable time separation is about $3t_*$ (figure 10), and the conditional average of uv, constructed from acceleration events, therefore has a peak at about that time. This is also true for the retardation events, although for this case the peak occurs after the detection time. The uv-pattern has, for both cases, only one peak. The double peak reported by Blackwelder & Kaplan (1976) has been interpreted as being caused by a 'strong' sweep following an ejection, but the present results show that it may be a result of not separating the two types of events. We found that only rarely is an ejection followed by a sweep with a large uv-peak, or *vice versa*. This was also noted by Rajagopolan & Antonia (1982).

Some uv-peaks do not correspond to events detectable in the u-signal (with the VITA technique), but occur in conjunction with strong activity in the v-component, especially during periods of low streamwise velocity. These events could be detected by applying the VITA technique to the v-signal (see e.g. event C in figure 5). A typical timescale (duration) of these events is a factor 2–3 smaller than that of the u-signal events (figure 6a). This is also reflected in the conditional averages of u and v obtained

with the uv-quadrant method for which the u-patterns are roughly a factor of 2 wider than the v-patterns.

The conditional averages of u, v and uv obtained with the uv-quadrant method all have their extreme values approximately at the detection time. As was shown in §2.1, the magnitude of the $\langle uv \rangle$-peak (and its dependence on H) can be predicted if the frequency of occurrence of events, as function of H, is known. Also for the VITA technique the extreme values of $\langle u \rangle$, $\langle v \rangle$ and $\langle uv \rangle$ coincide. However, this does not occur at the detection time where $\langle u \rangle$ and $\langle v \rangle$ are close to zero. The u- and v-patterns are approximately 180° out of phase for both methods. This was also found by Wallace *et al.* (1977) to be true for their pattern-recognition technique. The u-pattern obtained with their method is characterized by a period of low streamwise velocity followed by a rapid acceleration. Close to the wall ($y^+ < 15$) $\langle v \rangle$ changes sign somewhat earlier than $\langle u \rangle$, i.e. the flow is directed towards the wall before $\langle u \rangle$ becomes positive. This behaviour, which also can be seen in the data of Blackwelder & Kaplan (1976) at $y^+ = 15$, is usually termed wallward interaction. The conditional averages of similar wallward interaction events at $y^+ = 50$ (quadrant 3 in figure 12) exhibit a period of low streamwise velocity and a positive value of $\langle v \rangle$ before the detection. This may be interpreted in conjunction with the above-described behaviour.

As most events detected in the u-signal with the VITA technique are associated with ejections, the velocity patterns constructed from these events should, at least to some extent, correspond to those obtained with the uv-quadrant method in the second quadrant. The patterns obtained with the two methods, however, have quite different appearances. Visual inspection of long-time records suggested that the u-pattern obtained with the VITA technique gives the better representation of the actual realizations. This may be attributable to the fact that both acceleration and retardation type of VITA events, as well as VITA events detected in v, are associated with ejections. For instance, if hypothetically the ensemble averages of acceleration events (figure 7*b*) are added to those of retardations (figure 7*c*) with an appropriate time shift so that the uv-peaks coincide the resulting u- and v-patterns would show a closer resemblance to those obtained with the uv-quadrant method.

An interesting quantity obtainable with the uv-quadrant method is the mean duration of uv-peaks, which can be estimated from the width of $\langle uv \rangle$. This quantity is not easily obtainable with the VITA technique because of the influence of the averaging time. Our ensemble averages and those of Comte-Bellot *et al.* (1979) indicate that the mean duration of uv-peaks scales neither with the inner nor the outer timescale in the outer region. However, the frequency of occurrence scales with outer variables in this region, as does also the frequency of occurrence of VITA events, as shown by Johansson & Alfredsson (1982). A comparison between the mean duration of uv-peaks, in the near-wall region, for different Reynolds numbers, would yield valuable information on the governing timescale in this region. However, it is difficult to get a reasonably wide Reynolds-number range for such a comparison and still retain sufficient spatial resolution.

The sharp increase of the streamwise velocity at the detection time, which is characteristic for the acceleration events, may be interpreted as being caused by a shear layer passing the probe. The flow observed resembles qualitatively that described by the theoretical model of Landahl (1980). At the downstream side of the shear layer a region of low-speed fluid moves away from the wall, while, at the upstream side, a region of high-speed fluid approaches the wall at a rather small angle. The outflow angle for typical VITA events often exceeds 10° (see e.g. events *A* and

B in figure 5). Also, the ejection-events detected with the *uv*-quadrant method are, for large threshold levels, associated with large outflow angles. For instance, the angle inferred from the conditional averages in figure 13 is about 12°.

The work reported here is part of a research programme sponsored by the Swedish Maritime Research Centre (SSPA). We gratefully acknowledge this support. We also want to thank Professors M. T. Landahl and F. H. Bark for many fruitful discussions.

REFERENCES

ANTONIA, R. A. 1981 *Ann. Rev. Fluid Mech.* **13**, 131.

BLACKWELDER, R. F. & KAPLAN, R. E. 1976 *J. Fluid Mech.* **76**, 89.

BRODKEY, R. S., WALLACE, J. M. & ECKELMANN, H. 1974 *J. Fluid Mech.* **63**, 209.

CHAMPAGNE, F. H., SLEICHER, C. A. & WEHRMANN, O. H. 1967 *J. Fluid Mech.* **28**, 153.

CHEN, C. H. P. & BLACKWELDER, R. F. 1978 *J. Fluid Mech.* **89**, 1.

COMTE-BELLOT, G., SABOT, J. & SALEH, I. 1979 In *Proc. Dynamic Flow Conf., 1978, Marseille–Baltimore*, p. 213.

CORINO, E. R. & BRODKEY, R. S. 1969 *J. Fluid Mech.* **37**, 1.

ECKELMANN, H. 1970 *Mitteilungen aus dem MPI für Strömungsforschung und der AVA, Göttingen*, no. 48.

ECKELMANN, H., NYCHAS, S. G., BRODKEY, R. S. & WALLACE, J. M. 1977 *Phys. Fluids Suppl.* **20**, S225.

ECKELMANN, H. & WALLACE, J. M. 1981 In *The Role of Coherent Structures in Modelling Turbulence and Mixing* (ed. J. Jimenez). Lecture Notes in Physics, vol. 136, p. 292. Springer.

HOFBAUER, M. 1978 *Mitteilungen aus dem MPI für Strömungsforschung und der AVA, Göttingen*, no. 66.

JOHANSSON, A. V. & ALFREDSSON, P. H. 1981 *R. Inst. Tech., Stockholm, Rep.* TRITA-MEK-81-04 (ISSN 0348-467 X).

JOHANSSON, A. V. & ALFREDSSON, P. H. 1982 *J. Fluid Mech.* **122**, 295.

KIM, H. T., KLINE, S. J. & REYNOLDS, W. C. 1971 *J. Fluid Mech.* **50**, 133.

KLINE, S. J., REYNOLDS, W. C., SCHRAUB, F. A. & RUNSTADLER, P. W. 1967 *J. Fluid Mech.* **30**, 741.

KREPLIN, H.-P. & ECKELMANN, H. 1979*a* *Phys. Fluids* **22**, 1210.

KREPLIN, H.-P. & ECKELMANN, H. 1979*b* *Phys. Fluids* **22**, 1233.

LANDAHL, M. T. 1980 In *Proc. ICHMT/IUTAM Symp. on Heat and Mass Transfer and Structure of Turbulence, Dubrovnik, Yugoslavia.*

LU, S. S. & WILLMARTH, W. W. 1973 *J. Fluid Mech.* **60**, 481.

NYCHAS, S. G., HERSHEY, H. C. & BRODKEY, R. S. 1973 *J. Fluid Mech.* **61**, 513.

OFFEN, G. R. & KLINE, S. J. 1973 *Dept Mech. Engng, Stanford Univ., Rep.* MD-31.

RAJAGOPALAN, S. & ANTONIA, R. A. 1982 *Phys. Fluids* **25**, 949.

SUBRAMANIAN, C. S., RAJAGOPOLAN, S., ANTONIA, R. A. & CHAMBERS, A. J. 1982 *J. Fluid Mech.* **123**, 335.

TASLIM, M. E., KLINE, S. J. & MOFFAT, R. J. 1978 *Dept Mech. Engng, Stanford Univ., Rep.* TMC-4.

WALLACE, J. M., BRODKEY, R. S. & ECKELMANN, H. 1977 *J. Fluid Mech.* **83**, 673.

WALLACE, J. M., ECKELMANN, H. & BRODKEY, R. S. 1972 *J. Fluid Mech.* **54**, 39.

WILLMARTH, W. W. & BOGAR, T. J. 1977 *Phys. Fluids Suppl.* **20**, S9.

WILLMARTH, W. W. & LU, S. S. 1972 *J. Fluid Mech.* **55**, 65.